

# Enhanced Activity of Acetyl CoA Synthetase Adsorbed on Smart Microgel: an Implication for Precursor Biosynthesis

Nidhi Chandrama Dubey,<sup>†,‡</sup> Bijay Prakash Tripathi,<sup>†</sup> Martin Müller,<sup>†</sup> Manfred Stamm,<sup>†,‡</sup> and Leonid Ionov<sup>\*,†</sup>

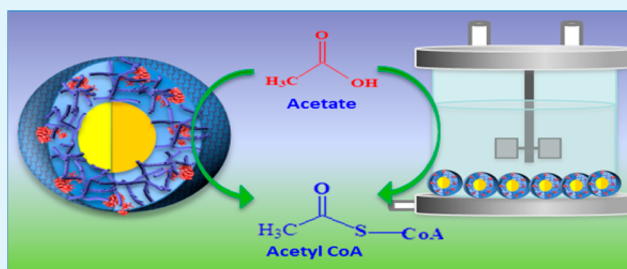
<sup>†</sup>Department of Nanostructured Materials, Leibniz-Institut für Polymerforschung Dresden e. V., Hohe Str. 6, D-01069 Dresden, Germany

<sup>‡</sup>Physical Chemistry of Polymer Materials, Technische Universität Dresden, Dresden 01069, Germany

## S Supporting Information

**ABSTRACT:** Acetyl coenzyme A (acetyl CoA) is an essential precursor molecule for synthesis of metabolites such as the polyketide-based drugs (tetracycline, mithramycin, Zocor, etc.) fats, lipids, and cholesterol. Acetyl CoA synthetase (Acs) is one of the enzymes that catalyzes acetyl CoA synthesis, and this enzyme is essentially employed for continuous supply of the acetyl CoA for the production of these metabolites. To achieve reusable and a more robust entity of the enzyme, we carried out the immobilization of Acs on poly(*N*-isopropylacrylamide)-poly(ethylenimine) (PNIPAm-PEI) microgels via adsorption. Cationic PNIPAm-PEI microgel was synthesized by one-step graft copolymerization of NIPAm and *N,N*-methylene bis-acrylamide (MBA) from PEI. Adsorption studies of Acs on microgel indicated high binding of enzymes, with a maximum binding capacity of 286  $\mu\text{g}/\text{mg}$  of microgel for Acs was achieved. The immobilized enzymes showed improved biocatalytic efficiency over free enzymes, beside this, the reaction parameters and circular dichroism (CD) spectroscopy studies indicated no significant changes in the enzyme structure after immobilization. This thoroughly characterized enzyme bioconjugate was further immobilized on an ultrathin membrane to assess the same reaction in flow through condition. Bioconjugate was covalently immobilized on a thin layer of preformed microgel support upon polyethylene terephthalate (PET) track etched membrane. The prepared membrane was used in a dead end filtration device to monitor the bioconversion efficiency and operational stability of cross-linked bioconjugate. The membrane reactor showed consistent operational stability and maintained >70% of initial activity after 7 consecutive operation cycles.

**KEYWORDS:** smart polymer, core-shell microgel, acetyl CoA synthetase, enzyme adsorption, acetyl CoA synthesis



## INTRODUCTION

Acetyl CoA is one of the vital biomolecules, which is metabolized to fulfill the energy demand of a living cell.<sup>1</sup> It plays a diverse role as a precursor molecule in synthesis of fatty acid, cholesterol, polyketide based drug, etc., and hence acetyl CoA has high demand for commercial synthesis of above molecules.<sup>2–4</sup> One of the main concerns in the synthesis of drugs and pharmaceutically important lipids is the high cost of the precursor molecule, and hence different in vitro chemical and enzyme-based acetyl CoA regeneration systems are employed to reassure the supply of this molecule.<sup>5–7</sup> The chemical approaches are not attractive because of the use of organic solvents for acylation of CoA, and moreover the reactions are not 100% specific. This makes in situ use of these systems difficult and beside this, for each turnover the batch extraction and acylation of CoA becomes necessary.<sup>8</sup> Therefore, enzymatic methods are favored over chemical methods. One such system is the use of enzyme acetyl CoA synthetase (Acs; acetate: CoA ligase, EC 6.2.1.1), which catalyzes the synthesis of acetyl CoA from acetate.<sup>5,8</sup> The main advantages of Acs is its

high substrate specificity, and the two step synthetic reaction of acetyl CoA is carried out by single enzyme system as shown in Figure 1.<sup>9–11</sup> Enzyme catalyzed reactions are considered as “Green” for sustainable technologies and are excellent catalyst

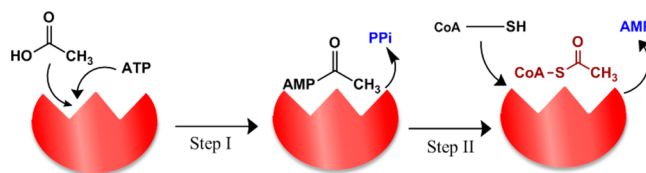


**Figure 1.** Two step reaction for acetyl CoA synthesis catalyzed by acetyl CoA synthetase (Acs). Step I: Acetate is activated to acetyl-AMP in the presence of ATP at lysine residue of enzyme active site with release of pyrophosphate (PPi). Step II: Marks the synthesis of acetyl CoA from CoA and acetyl AMP.

**Received:** September 17, 2014

**Accepted:** January 5, 2015

**Published:** January 5, 2015

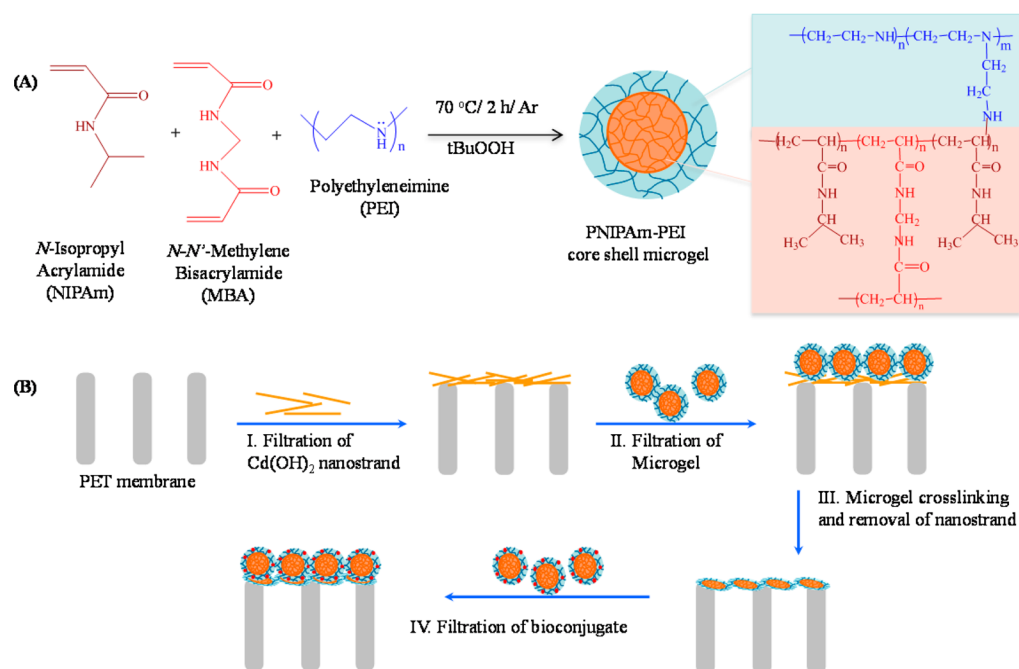


**Figure 2.** (A) Scheme for synthesis of the PNIPAm-PEI microgel. (B) Schematic for bioconjugate modified membrane preparation.

due to their high activity, selectivity, and specificity, by virtue of which they are able to perform complex chemical processes under experimental and environmental benign conditions.<sup>12,13</sup> Beside being an excellent catalyst, enzyme implementation for industrial application has to surpass stability and activity challenges in given reaction conditions.<sup>14</sup> Immobilization of enzymes improves the process economics by enabling multiple uses of catalyst and improving overall productivity and robustness.<sup>12,14–16</sup> Until now glass beads,<sup>17,18</sup> Nafion membrane,<sup>19</sup> cellulose fiber,<sup>20</sup> and Sepharose 4B<sup>21</sup> had been used for acetyl CoA synthetase attachment. Our group has previously reported immobilization of Acs on cationic thermo responsive PNIPAm-AEMA microgel by covalent coupling, where we were able to reuse the bioconjugate for 4 consecutive cycles with more than 50% activity.<sup>22</sup> A more versatile and enzyme friendly approach is necessary for sustainable synthesis of acetyl CoA.

Nano and submicron smart polymer particles have been explored extensively for immobilization and process optimization in the field of biocatalysis due to their size dependent properties, which provide a high interface with the surrounding medium.<sup>23–27</sup> These particles, when prepared with core-shell morphology, provide advantages of two component system: one in principle forms the core and another forms the shell of the particles.<sup>28</sup> With advanced research in the synthesis of core-shell particles, it is possible to design well-defined particles to match the process requirement.<sup>29,30</sup> Smart polymers like PNIPAm are one of the extensively studied thermoresponsive materials because of its pronounced thermal response near physiological temperature and well-standardized synthetic protocols.<sup>31–33</sup> Many enzymes (trypsin,<sup>34–36</sup> lysozyme,<sup>37,38</sup> etc.) had been immobilized on PNIPAm microgel, and temperature dependent activities and switching of bioconjugates were studied. Detailed work from the Ballauff group on core-shell PNIPAm-PS particles had proven microgel as a good support for biocatalyst.<sup>26,39,40</sup> In addition to this, particles coated with a bed of ionic polymers provide a large density of ionic groups that can interact strongly with charged patches on

enzyme via ionic exchange.<sup>41,42</sup> If the enzyme to be immobilized can penetrate into the large and flexible ionic polymer bed on the particles, a high level of stabilization can be achieved for the multimeric enzyme by fixing it into the support through large number of connections.<sup>42,43</sup> Likewise PEI is a cationic polymer and is well-known as a stabilizing agent for enzymes.<sup>44,45</sup> It provides multiple attachment points for the enzyme and thus protects its quaternary structure.<sup>44,46</sup> Core-shell microgels prepared from both these polymers acquire better dual properties of stimuli-responsiveness and enzyme stabilization in a single system.<sup>47</sup> Such microgels had been previously used by other groups to synthesize gold nanoparticles and subsequently immobilize enzymes on the nanoparticles.<sup>48</sup> These microgels can also be further utilized to fabricate thin films and membranes for obtaining functional surfaces.<sup>23</sup> These works encourage us for further investigation of the PNIPAm-PEI microgel system for study of interactions of the microgel with the enzyme and its end application.

In this paper, we report Acs immobilization on thermo responsive PNIPAm-PEI core-shell microgels via ionic adsorption and explore the potential of bioconjugate for acetyl CoA synthesis in a membrane reactor. Details of the quantitative study on enzyme activity and structural characteristics of the enzyme after immobilization is presented. Further an ultrathin membrane is fabricated to assess the acetate conversion and operational stability in flow through conditions.

## EXPERIMENTAL SECTION

**Materials and Methods.** *N*-Isopropylacrylamide (97%; NIPAm) was purified by recrystallization in *n*-hexane. Branched poly(ethylenimine) (PEI) with an average molecular weight of 25 000 (50 wt % solution in water), *N,N*-methylene bis(acrylamide) ( $\geq 99.5\%$ ; MBA), *tert*-butyl hydroperoxide (70% solution in water, *t*BuOOH), *S*-acetyl-coenzyme A synthetase (Acs; E C 6.2.1.1,  $>3$  units/mg, from baker's yeast), malic acid dehydrogenase (Mdh) from porcine heart ( $\geq 600$  units/mg protein), citrate synthase (Cs) from porcine heart ( $\geq 100$  units/mg protein), and all other chemicals were obtained from Sigma-Aldrich (Germany). BCA Protein Assay Kit (Thermo scientific

(Pierce protein)), acetyl coenzyme A (Roche, Germany),  $\beta$ -nicotinamide adenine dinucleotide, NADH disodium salt (Carl Roth, Germany), and 30 kDa MWCO centrifugal filter tubes (Millipore) were purchased from respective suppliers. The polyethylene terephthalate (PET) track etched micro porous membranes (diameter: 47 mm, pore size: 0.3–0.4  $\mu\text{m}$ , pore density:  $1.5 \times 10^8$  pores/cm<sup>2</sup>) were obtained from it4ip, Belgium.

**Synthesis of PNIPAM-PEI Core–Shell Microgels.** The cationic thermoresponsive PNIPAm-PEI microgel was synthesized via graft copolymerization of NIPAm and MBA from PEI (Figure 2A).<sup>47</sup> The molar ratios of monomer, cross-linker, and functional polymer in 50 mL reaction mixture were as follows: 0.141 mol/L NIPAm (93%), 0.0103 mol/L MBA (6.8%), and 0.000016 mol/L PEI (0.2%). Polymerization was carried out in a three-necked round bottomed flask equipped with a reflux condenser, a thermometer, and argon inlet under continuous magnetic stirring (300 rpm). A mixture of NIPAm monomer (800 mg) and MBA (80 mg) in water were added to the flask, and the solution was treated with a gentle stream of argon for 30 min. Subsequently, PEI (0.4 g) was dissolved in water and the solution was neutralized to pH 7 using 1 M HCl solution. The PEI solution was then mixed with the monomer solution (total volume 50 mL) and the solution was heated to 70 °C under a gentle stream of argon. After the desired temperature of the solution was reached, diluted tBuOOH solution in water (0.5 mL, 10 mM) was added dropwise to the mixture to initiate polymerization reaction, and the reaction was allowed to proceed for 2 h, at 70 °C with constant stirring under argon atmosphere. After the completion of the reaction, the dispersion of microgels was carefully purified by repeated centrifugation at 13 000 rpm for 30 min and further purified by dialyzing against water using dialysis tubing (Cellulose membrane; 14 000 Da molecular weight cutoff) for 1 week at room temperature. Lyophilized microgel was dispersed to a concentration of 1 wt %. The microgel suspensions were shaken for 24 h to get an evenly dispersed microgel solution.

**Adsorption Experiment.** The immobilization of Acs on the PNIPAm-PEI microgel was achieved via adsorption in 0.1 M tris-Cl buffer at pH 8 for 6 h at 4 °C. The conjugate was obtained by centrifugation at 12 000 rpm for 15 min at 25 °C and subsequently washed with the same buffer to remove nonadsorbed enzymes. Using BCA (for protein concentrations 20–2000  $\mu\text{g}/\text{mL}$ ) assay kits the amounts of adsorbed enzyme loaded to microgel were determined by blanking out the microgel absorbance from the enzyme-microgel bioconjugate. The enzyme and conjugate were stored in 0.1 M tris buffer (pH 8) containing 1 mM glutathione (an antioxidant) and 1 mM magnesium chloride (divalent cation)<sup>49</sup> for further use.

**Enzyme Activity Assay.** The activity of free and immobilized Acs was determined spectro-photometrically by following acetyl CoA synthesis at 340 nm by coupling with citrate synthase (Cs) and malate dehydrogenase (Mdh) assay in a 96 well format. The assay medium composition for enzyme activity consisted of 20 mM potassium acetate, 4 mM MgCl<sub>2</sub>, 4 mM glutathione, 1 mM ATP, 500  $\mu\text{M}$  coenzyme A, 1 mM NAD<sup>+</sup>, 4 mM malate, 16.6 U/mL Mdh, and 5 U/mL Cs in 100 mM tris-Cl buffer at pH 8. The interference from microgel solution was blanked out for all the measurements. The acetyl CoA synthesized was correlated to the concentration of NADH formed in the coupled assay using  $\epsilon_{340} = 0.6220 \text{ M}^{-1} \text{ cm}^{-1}$ . One unit of enzyme activity was defined as the amount of enzyme which is required to form 1  $\mu\text{mol}$  of NADH per min at pH 8 and 37 °C.<sup>50</sup> The temperature dependent enzyme activities of immobilized and free enzymes were studied from 25 to 65 °C in 100 mM tris-Cl buffer at pH 8. The effect of pH on enzyme activities was studied for the pH range 6–9 at 37 °C in the respective buffers 0.1 M phosphate buffers (pH 6, 6.5, 7, and 7.5) and 0.1 M tris-Cl buffer (pH 8, 8.5 and 9). Kinetic parameters of enzymes were determined by varying acetate concentration (0.3–5 mM) while keeping concentrations of ATP and CoA constant at 1 mM and 0.5 mM, respectively. The activity of enzymes was studied in triplicate, and the standard deviation was used as the error.

**Enzyme Immobilized Membrane Fabrication.** The enzyme immobilized ultrathin membrane surface was prepared on a PET track etched membrane support using enzyme-immobilized microgels. The

membrane fabrication strategy is outlined in Figure 2B. The pores of the PET membrane were first covered with Cd(OH)<sub>2</sub> nanostrands, which were prepared by mixing CdCl<sub>2</sub> and aminoethanol solution.<sup>51</sup> An aqueous solution of 0.3 mM 2-aminoethanol was quickly mixed under stirring with an equi-volume of 4 mM cadmium chloride and allowed to stand for 30 min to form cadmium hydroxide nanostrands. The nanostrand solution (10 mL) was suction filtered on the PET membrane. Subsequently, a thin layer of microgels was prepared by filtering a 0.2 mg/mL microgel solution and cross-linked by glutaraldehyde. After microgel cross-linking, the sacrificial cadmium hydroxide nanostrand layer was removed by passing of 10 mM HCl solution and washing with water. 100  $\mu\text{L}$  of the enzyme immobilized microgels was diluted in 0.1 M tris-Cl buffer (pH 8) to 1 mL and poured on the cross-linked microgel surface to covalently attach with free aldehyde groups for 30 min at 4 °C. Further suction filtration was carried out to fix the bioconjugate on the membrane, uncross-linked bioconjugate was removed by washing and the final membrane was used in dead end filtration device to check the catalytic performance.

The permeation behavior of the prepared microgel-based membrane was evaluated by measuring the pure water flux under the pressure range from 1 to 4 bar. The catalytic activity of the membrane was evaluated by determining the acetyl CoA formation at different time points for the enzyme immobilized on the membrane and free enzyme activity at 25 °C. For this purpose the reactants were supplied to dead end filtration device and permeate was collected at definite time intervals. The reaction buffer composition consists (total volume 4 mL) of 5 mM potassium acetate, 4 mM MgCl<sub>2</sub>, 4 mM glutathione, 50  $\mu\text{M}$  ATP, and 50  $\mu\text{M}$  coenzyme A, in 100 mM tris-Cl buffer at pH 8 and further acetyl CoA formed was assayed with 0.5 mM NAD<sup>+</sup> 2.5 mM malate, 16.6 U/mL Mdh, and 5 U/mL Cs in Tris buffer pH 8. Furthermore, the operational stability or the reusability of the membrane was checked for consecutive reaction cycles with 1 mL of the reaction buffer under similar assay conditions. After each cycle the membrane was washed 2–3 times with a total of 5 mL of 0.1 M tris-Cl buffer containing 10% glycerol, 1 mM glutathione, and 1 mM MgCl<sub>2</sub> to remove any entrapped reactant or product.

**Characterization Techniques.** *Dynamic Light Scattering and Zeta Potential.* The dynamic light scattering (DLS) measurements under different temperatures were performed for the microgel to analyze the particle size and its thermoresponsive behavior. Zeta potential measurements of particles were also carried out to identify the charge behavior with respect to pH. Both, DLS and zeta potential experiments were done using Zetasizer Nano ZS (Malvern Instruments, U.K.), equipped with a 633 nm He/Ne laser and noninvasive back scatter (NIBS) technology. Before the size measurements, samples were thermally equilibrated for 10 min, and data were acquired by averaging 30 measurements, with a 10 s integrating time for each measurement. The volume phase transition temperature was determined with respect to temperature (24–40 °C). The zeta potential was obtained from the pH range 6–11 and the values were an average of three successive readings.

*Atomic Force Microscopy (AFM).* The surface topography and height of the dry microgel was imaged using a Nanoscope III Multimode atomic force microscope (Digital Instruments, Santa Barbara, CA) in tapping mode.

*Scanning Electron Microscopy.* SEM was performed on vacuum-dried microgels on a silicon wafer and a microgel-bioconjugate film on PET membrane using a NEON 40 FIB-SEM workstation (Carl Zeiss AG, Germany) operated at 3 kV, after 3 nm thick sputter coating of platinum.

*Circular Dichroism Spectra.* UV-CD spectra of native and desorbed Acs were measured on a Jasco 810 (Jasco, Germany) using a quartz cuvette with 1 mm path length. Spectra were corrected by subtracting the buffer baseline. CD spectroscopy was applied to examine the secondary structure of the proteins. The spectra (190 to 250 nm) were analyzed using the tool “CD-PRO-Analysis” of Jasco Software Spectra Manager Version 2 (Version 2.06.00 [Build 6]) from JASCO GmbH, Groß-Umstadt, Germany.

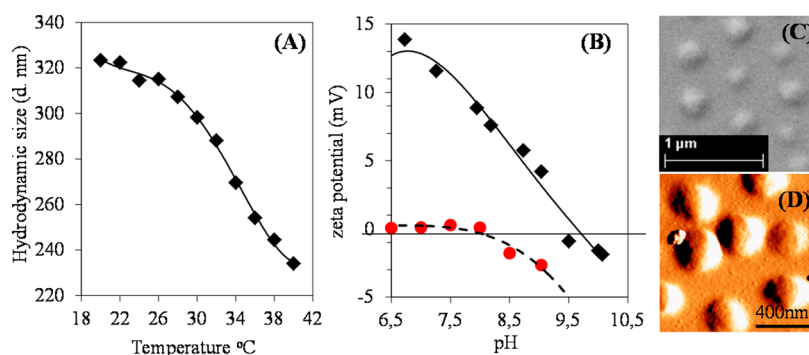


**Figure 3.** Characterization of the PNIPAm-PEI microgel: (A) dynamic light scattering measurement of the microgel (0.01 mg/mL in water) and the plot describe the change in hydrodynamic size as a function of temperature. (B) Zeta potential of PNIPAm-PEI microgel (black square) and bioconjugate (red circle) as a function of pH; and (C and D) SEM and AFM images of the PNIPAm-PEI core-shell microgel.

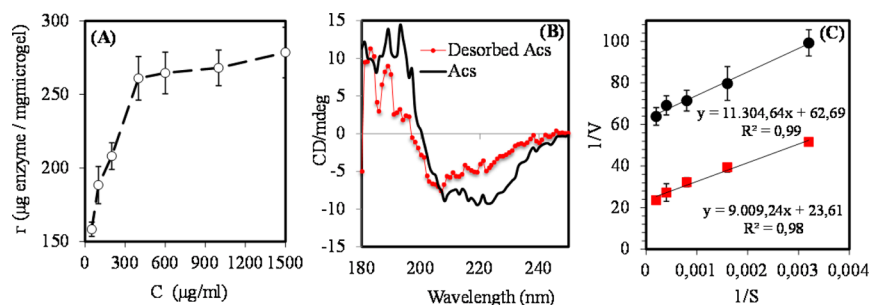


**Figure 4.** (A) Acs adsorption isotherm: The adsorbed amount of Acs per mg of microgel ( $\Gamma$ ) is plotted versus the concentration of free enzyme in solution ( $C$ ). (B) Circular dichroism spectra for free Acs and desorbed Acs in 0.01 M potassium phosphate solutions (pH 4) at 37 °C (protein concentration 0.05 mg/mL). (C) Lineweaver-Burk plots for acetate conversion to acetyl CoA by immobilized (red square) and native Acs (black circle) at 37 °C.

## RESULTS AND DISCUSSION

**Synthesis of PNIPAM-PEI Microgels.** The microgels were prepared by graft copolymerization of the NIPAM and MBA from the PEI in the presence of initiator *t*-BuOOH in aqueous media. The initiator reacts with the amino group on the PEI chains and generates amino and *t*-BuOO<sup>−</sup> free radicals. These free radicals simultaneously initiate graft copolymerization and homopolymerization of the NIPAM in the presence of the cross-linker, MBA. As the polymerization was performed above the lower critical solution temperature (LCST) of PNIPAm, in this condition the newly formed PNIPAm chains are in a collapsed state due to hydrophobic interactions, whereas the PEI chains remain hydrophilic. These amphiphilic PEI-g-PNIPAM act as a polymeric-surfactant that self-assembles into a micelle like microdomain and continues to promote emulsion polymerization of NIPAM. This results in colloidal microgels with PNIPAm core and PEI shell.<sup>45,47</sup> This method of synthesis gives a high rate of monomer conversion, and a high molar amount of cross-linker yields a microgel with a dense core.<sup>47,52</sup> The prepared microgels were then probed for their size and morphological characteristics. The dynamic light scattering measurement of the microgel is depicted in Figure 3A, The plot of the size of the microgels versus temperature demonstrate its thermoresponsive property; the size of microgels in water at 24 °C was found to be 320 nm, while at 40 °C, the size reduced to 234 nm. The PNIPAm microgels possess a volume phase transition from a swollen state to a collapsed state at or near the cloud point of PNIPAm (32 °C),<sup>53</sup> and this transition temperature tends to shift in the presence of functional comonomer in the structure.<sup>31,53</sup> The PNIPAm-PEI microgel exhibits the volume phase transition

temperature (VPTT) at around 32 °C which is near to the LCST of PNIPAm, confirming that the transition temperature was not affected by the copolymer. The zeta potential measurement of the microgel as a function of pH is depicted in Figure 3B. The zeta potential for the microgel was positive at a wide range of pH, and the isoelectric point of the microgel was found to be around 10. These results indicate that the cationic microgels were synthesized and the positive charge was contributed from the PEI polymer to the microgel structure. The morphological characteristics of dried microgels were imaged with the help of SEM and AFM technique and are depicted in Figure 3C,D. It is evident from the microscopic images that the microgels were highly monodispersed and are about 250 nm in size.

**Adsorption of Acetyl CoA Synthetase on the PNIPAm-PEI Microgel.** Preliminary experiments were performed to determine optimal conditions like pH, temperature, and microgel concentration for enzyme coupling. The adsorption studies were then performed at standard conditions of temperature (<10 °C) and pH (8.0) using the microgel solution (10 mg/mL). The adsorption isotherm studies were carried by investigating the Acs binding to microgel as a function of enzyme concentrations. Figure 4A suggest the adsorption behavior of Acs on microgel follows a Langmuir-type model, which can be described by the following Langmuir isotherm (eq 1):<sup>54</sup>

$$\Gamma = \frac{\Gamma_{\max} C}{K_d + C} \quad (1)$$

The Langmuir isotherm equation can be linearized by multiplying both sides by ( $K_d + C$ ) and further dividing by  $\Gamma$ ,

and this results in eq 2 with which the experimental data were fit:

$$\frac{C}{\Gamma} = \left( \frac{1}{\Gamma_{\max}} \right) \left( C + \frac{K_d}{\Gamma_{\max}} \right) \quad (2)$$

where  $\Gamma$  is the amount of Acs adsorbed on the microgel ( $\mu\text{g}/\text{mg}$ ),  $\Gamma_{\max}$  is the maximum binding capacity ( $\mu\text{g}/\text{mg}$ ),  $c$  is the Acs concentration in solution ( $\mu\text{g}/\text{mL}$ ), and  $K_d$  is the dissociation constant ( $\text{mL}/\mu\text{g}$ ). From the equation,  $K_d$  and  $\Gamma_{\max}$  were calculated to be  $0.019 \text{ mL}/\mu\text{g}$  and  $286 \mu\text{g}/\text{mg}$  of microgel, respectively. The maximum amount of enzyme adsorbed at the standardized conditions on the microgels was  $278 \mu\text{g}/\text{mg}$ , and this value was found to be close to the maximum binding capacity of microgels. These results indicate that a high load of enzymes on the microgel particles was achieved. The linear graph of enzyme adsorption showed excellent fit with relatively high  $R^2$  values (0.99) further confirming that the model predicts well with the adsorption behavior. The respective concentration of enzyme at which a maximum enzyme load was obtained was used to prepare the bioconjugate and was subsequently subjected to further studies. The PNIPAm-PEI microgel can be viewed as a support covered with a flexible ionic polymer (PEI) bed.<sup>41</sup> The PEI shell provides multiple sites for the attachment of enzymes that interact with various charged sites on the enzyme surface and hence stabilizes the enzyme and its subunits from denaturation and dissociation, respectively.<sup>42,46</sup> Since the adsorption was carried out at pH 8, which is close to the isoelectric point of Acs (pH 7.5), the overall charge on the microgel is positive due to protonated amino group of PEI shell.<sup>45,55</sup> The adsorption of Acs on the microgel occurs due to the ionic exchange between these anionic and cationic groups of respective molecules.<sup>42</sup> This assumption was confirmed by zeta potential results, and from Figure 3B it can be seen that a high positive zeta potential value of the microgel (8.87 mV) was significantly reduced after immobilization of Acs (0.0841 mV). Furthermore, the temperature for adsorption was below the cloud point or LCST of PNIPAm, and this finally states that the strong binding of the enzyme on microgel particles occurs in the swollen state of the microgel.<sup>40,46</sup>

**Circular Dichroism Study.** The conformational stability of enzymes after immobilization was studied using CD spectroscopy. The experiment with the enzyme loaded on the microgel was not successful due to a high interference from microgel particles.<sup>56</sup> Therefore, we subjected the enzyme that was desorbed from the microgel in 0.01 M potassium phosphate solutions (pH 4) at 37 °C for this study. Figure 4B shows CD spectra of free enzymes and enzymes desorbed from PNIPAm-PEI under the same conditions. The spectra obtained were then analyzed using Jasco Software Spectra Manager Version 2 (Jasco GMBH, Groß-Umstadt, Germany), and the respective secondary structure contributions are given in Table 1. The free enzyme possessed 48% of an  $\alpha$ -helical structure, which reduced to 35% of for immobilized Acs. These results show that nearly

**Table 1. Contribution of Secondary Structural Elements in Acs Estimated from CD Spectra**

	$\alpha$ -helical (%)	$\beta$ -sheet (%)	turn (%)	unordered (%)
free enzyme	48.8	6.4	20.8	24
immobilized enzyme	35	12.3	19.5	34.6

72% of the native structure of the enzyme was retained after immobilization. Further correlating these results with immobilization output of the bioconjugate, it was found that the conjugate possessed nearly 60% of the initial activity of the enzyme added to prepare the bioconjugate, which almost corresponds to the amount of enzyme immobilized on the microgel. Therefore, from these results it can be concluded that, though there were structural changes (indicated by CD spectroscopy) in the enzyme after immobilization, it had no adverse effect on the activity of the enzyme.

**Acs Reaction Kinetics.** The reaction kinetics of free and immobilized enzymes were studied at various concentrations of acetate (5 to 0.3 mM) as a substrate while keeping the ATP and CoA concentrations constant (1 and 0.5 mM, respectively). The dependence of the initial rate on the substrate concentration was measured and the experimental data were analyzed by Lineweaver–Burk plots. The two important kinetic parameters, Michaelis constant  $K_m$  and turn over number  $k_{\text{cat}}$ , were calculated from linear regression curves (Figure 4C) and are represented in Table 2. The  $K_m$  values for immobilized

**Table 2. Kinetic Parameters of Immobilized and Free Enzyme for Acetate Substrate at 37 °C**

enzyme	$K_m$ (mM)	$k_{\text{cat}}$ ( $\text{s}^{-1}$ )	$k_{\text{cat}}/K_m$ ( $\text{mM}^{-1} \text{ s}^{-1}$ )
immobilized enzyme	$0.42 \pm 0.01$	$580 \pm 29$	1381
free enzyme	$0.18 \pm 0.02$	$205 \pm 16$	1139

enzyme were higher compared to those for free enzyme, which indicates a decrease in substrate–enzyme binding affinity. The  $K_m$  value for free enzyme obtained was close to the earlier report on Acs from yeast.<sup>57</sup> The increase in  $K_m$  after immobilization on charged particles is expected, as the carrier plays an important role in availability of the substrate to the enzyme. Steric hindrance, interaction with substrate, and the diffusion barrier contribute to the low availability of substrate near the active site of the enzyme.<sup>43</sup> By virtue of these effects, a high amount of substrate is required to attain the maximum rate of reaction and hence contributing to higher value of  $K_m$  compared to that of free enzyme. On the other hand, a positive effect was observed on turn over number ( $k_{\text{cat}}$ ) which shows a significant increase, marked by  $\sim 3$  times higher  $k_{\text{cat}}$  compared to the free enzyme. This indicates that the enzyme–substrate complex is moreover directed toward product formation. In our previous report on Acs immobilization on the AEMA-PNIPAm microgel, though there was no significant change in  $K_m$ , the rate of reaction was reduced by 34%.<sup>22</sup> From these values specificity constant ( $k_{\text{cat}}/K_m$ ) for free and immobilized enzymes were calculated to check the catalytic efficiency of enzymes.<sup>58</sup> Here also we found that the value for the immobilized enzyme stands better than the free enzyme, which further states the PEI–PNIPAm microgel as a superior carrier for Acs immobilization.

**Effect of Temperature and pH on Acs Activity.** The temperature and pH have a profound effect on the activity of enzymes, and study on the effect of these parameters on the activity of enzymes points out the changes in conformation of the enzyme on binding to the support.<sup>54</sup> In the current work, the enzymes were subjected to temperature dependent study in the range of 25–65 °C and reaction was carried out for 15 min. It is clear from Figure 5A that the activity of both the immobilized and free Acs exhibit temperature dependence. The free enzyme had a maximum activity at 37 °C which is similar to literature value and the activity decreased upon further

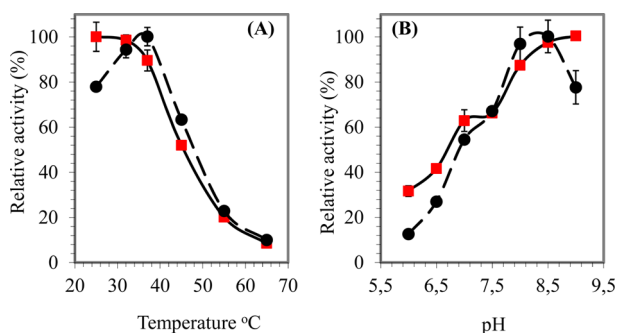


**Figure 5.** Effect of (A) temperature and (B) pH on the activities of free (●, dashed lines) and immobilized Acs (red square, solid lines).

increase in the temperature.<sup>55</sup> The results also shows that immobilized enzymes showed higher activity at temperatures below the LCST of PNIPAm (32 °C) and the activity gradually decreased with increase in the temperature. The loss in enzyme activity signifies a decrease in the active enzyme concentration on the microgel. With the increase in temperature the microgel core structure collapses which leads to removal of enzymes and also entrapment of remaining enzymes within the polymer network in microgel blocking the substrate accessibility.<sup>59</sup> Furthermore, the similar thermal profile at a higher temperature of immobilized and free enzymes indicates that the native enzyme structure is maintained after adsorption to the microgel.

Activity of enzyme as a function of pH was studied from the pH range 6–9, and the properties of the immobilized enzyme were compared with those of the free enzyme. It can be seen in Figure 5B that the free enzyme has an optimal pH between 8.0 to 8.5, which is close to a previous report on Acs from yeast,<sup>55</sup> while immobilized Acs showed higher activity at pH 9. The shift in optimum pH is attributed to charged support, which often leads to displacements in the pH activity profile of immobilized enzymes. As pH is govern by H<sup>+</sup> and OH<sup>-</sup> ions in the solution, the PEI shell of the microgel leads to unequal partitioning of these ions between the microenvironment of the immobilized enzyme and the bulk phase.<sup>60,61</sup>

**Fabrication, Bioconversion, and Operational Stability of Membrane Bioreactor.** The enzyme membrane reactor serves as a good platform for biocatalysis and bioseparation. The membrane directs the mass transport across itself thus keeping the enzymes inside the reactor and also achieving some level of product separation. Moreover the continuous removal of product will maintain the equilibrium of a reaction toward the product side, thereby improving the productivity of the whole process, which is an exceptional advantage of the membrane reactor.<sup>14</sup> Keeping the above facts in mind, an enzymatic membrane reactor was constructed by covalently anchoring the immobilized enzyme-microgel bioconjugate on microgel-PET support. The membrane characterization using SEM and the flux data are described in the Supporting Information (Figure S1). The membrane performance was studied in stirred conditions and respective activity was compared to free enzyme (FE) and conjugate (CB) in batch mode. Using eq 3, the percent yield was calculated for FE, CB and CM. The “actual yield” is the acetyl CoA formed (determined by correlating with the coupled assay) to the “theoretical yield”, i.e., the expected acetyl CoA formed from 0.05 mM CoA, in the presence of 0.05 mM ATP and 5 mM acetate as cosubstrate.

$$\text{yield}(\%) = \frac{\text{actual yield}}{\text{theoretical yield}} \times 100 \quad (3)$$

The plots for acetyl CoA formed with respect to time for FE and conjugate CB in batch mode and conjugate on the membrane is depicted in Figure 6A. In the batch conditions, the

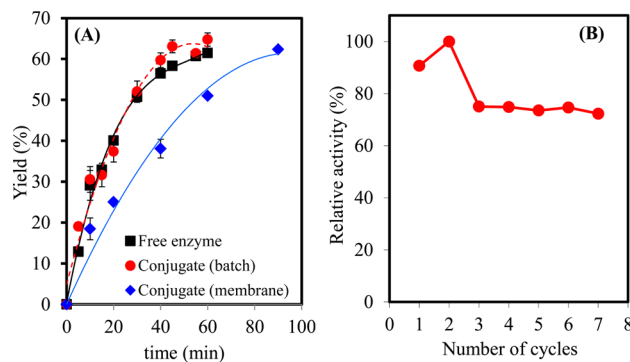


**Figure 6.** (A) Acetyl CoA formation is given as percent yield with respect to time by free Acs (■) and conjugate (red circle) in batch condition and conjugate on the membrane (blue diamond) at 25 °C. (B) Operational stability of bioconjugate membrane at 25 °C.

acetyl CoA formation was similar for both FE and CB, and the conversion reaction was linear until 40 min of reaction; thereafter the saturation limit was attained as depicted by a plateau. Whereas the membrane immobilized conjugate (CM) maintained the linear trend of product formation until the end of the reaction. The comparatively low amount of product formed in the case of CM with respect to FE and CB can be attributed to the diffusion limitation and unavailability of enzyme toward the membrane surface.<sup>14,43,62</sup> The initial rate of reaction was found to be 1.42, 1.69, and 0.68 μM/min for FE, CB, and CM, respectively, from nearly 2 U/mL activity of the enzymes. Our result can be positively comparable with the previously reported acetyl CoA formation using immobilized Acs, where Mannens et al. had reported complete 1 μM acetate conversion in 1–2 min time using 6.12 U reactor column reactor.<sup>17</sup> At the end of the reaction, the calculated percent yield was FE (61.5 ± 0.37%), CB (64.76 ± 3.41%), and CM (62 ± 0.1%). Additionally the storage stability of the membrane reactor was checked, for which the membrane was stored in the refrigerator (~4 °C) and on the fourth day of storage the enzyme possessed >50% of initial activity.

To study the efficacy of immobilized enzyme as a reusable biocatalyst for acetyl CoA synthesis, the membrane was subjected for operation stability studies. The catalyst reusability was determined by measuring the stability of the enzyme on the membrane reactor as a function of number of reuses. Consecutive reaction cycles were operated with alternate washing steps. The residual activity after each cycle is depicted in Figure 6B. The membrane showed consistent performance and maintained >70% initial activity of bioconjugate until the last cycle. Previously we could only achieve >50% initial activity after 4 operation cycles for Acs covalently immobilized on PNIPAm-AEMA microgel.<sup>22</sup> The better and consistent performance of the enzyme reactor can be attributed to the stabilizing effect of the PEI shell of the microgel on enzyme and also the membrane, which maintain the total enzyme concentration on the surface.

## CONCLUSION

In this study, the PNIPAm-PEI microgel was investigated as a support for Acs immobilization for acetyl CoA synthesis. High adsorption of enzyme was obtained due to strong ionic interaction between the PEI shell and the enzyme. The adsorption of the enzyme to the microgel improved the catalytic efficiency over the free enzyme. Enzyme parameters and conformation studies demonstrated the maintenance of structural integrity of the enzyme after immobilization. The bioconjugate was used to fabricate a thin biocatalytic membrane and the conversion was monitored in flow through operation condition. The membrane reactor gave consistent performance maintaining more than 70% of initial activity after multiple usage and high rate bioconversion of acetate with respect to time. These results suggest that the prepared membrane serve as a good platform for acetyl CoA synthesis and can be explored for other precursor biomolecule production.

## ASSOCIATED CONTENT

### Supporting Information

SEM image of the ultrathin bioconjugate-membrane on PET track etched support. Permeability results (flux versus pressure) of bioconjugate-microgel PET membrane using PBS buffer. This material is available free of charge via the Internet at <http://pubs.acs.org>.

## AUTHOR INFORMATION

### Corresponding Author

\*E-mail: [ionov@ipfdd.de](mailto:ionov@ipfdd.de). Fax: +49-3514658281. Tel: +49-3514658271.

### Author Contributions

The manuscript was written through contributions of all authors. All authors have given approval to the final version of the manuscript.

### Notes

The authors declare no competing financial interest.

## ACKNOWLEDGMENTS

We thank Ms. A. Caspari and Dr. C. Bellman for assisting in DLS and zeta potential measurements. The authors are grateful to Drs. M. Maitz and M. Tsurkan for allowing the use of instrumental facilities. B.P. Tripathi acknowledges the Alexander von Humboldt Foundation for AvH Postdoctoral Fellowship.

## REFERENCES

- (1) Nelson, D. L.; Cox, M. M. In *Lehninger Principles of Biochemistry*, 4th ed.; W. H. Freeman & Co. Malinon: New York, 2005.
- (2) Lian, J.; Si, T.; Nair, N. U.; Zhao, H. Design and Construction of Acetyl-CoA Overproducing *Saccharomyces cerevisiae* Strains. *Metab. Eng.* **2014**, *24*, 139–149.
- (3) Staunton, J.; Weissman, K. J. Polyketide Biosynthesis: a Millennium Review. *Nat. Prod. Rep.* **2001**, *18*, 380–416.
- (4) Go, M. K.; Chow, J. Y.; Cheung, V. W. N.; Lim, Y. P.; Yew, W. S. Establishing a Toolkit for Precursor-Directed Polyketide Biosynthesis: Exploring Substrate Promiscuities of Acid-CoA Ligases. *Biochemistry* **2012**, *51*, 4568–4579.
- (5) Kim, M. I.; Kwon, S. J.; Dordick, J. S. In Vitro Precursor-Directed Synthesis of Polyketide Analogues with Coenzyme A Regeneration for the Development of Antiangiogenic Agents. *Org. Lett.* **2009**, *11*, 3806–3809.
- (6) Wu, H.; Tian, C.; Song, X.; Liu, C.; Yang, D.; Jiang, Z. Methods for the Regeneration of Nicotinamide Coenzymes. *Green Chem.* **2013**, *15*, 1773–1789.
- (7) Zhao, H.; van der Donk, W. A. Regeneration of Cofactors for Use in Biocatalysis. *Curr. Opin. Biotechnol.* **2003**, *14*, 583–589.
- (8) Woodyer, R. D.; Johannes, T. W.; Zhao, H. Regeneration of Cofactors for Enzyme Biocatalysis, in *Enzyme Technology*; Pandey, A., Webb, C., Soccol, C. R., L. C., Ed.; Springer science: Delhi, 2006; pp 85–104.
- (9) Patel, S. S.; Walt, D. R. Substrate Specificity of Acetyl Coenzyme A Synthetase. *J. Biol. Chem.* **1987**, *262*, 7132–7134.
- (10) Jogl, G.; Tong, L. Crystal Structure of Yeast Acetyl-Coenzyme A Synthetase in Complex with AMP. *Biochemistry* **2004**, *43*, 1425–1431.
- (11) Gulick, A. M.; Starai, V. J.; Horswill, A. R.; Homick, K. M.; Escalante-Semerena, J. C. The 1.75 Å Crystal Structure of Acetyl-CoA Synthetase Bound to Adenosine-5'-propylphosphate and Coenzyme A. *Biochemistry* **2003**, *42*, 2866–2873.
- (12) Sheldon, R. A. Enzyme Immobilization: The Quest for Optimum Performance. *Adv. Synth. Catal.* **2007**, *349*, 1289–1307.
- (13) Guisan, J. M. *Immobilization of Enzymes and Cells*, 2nd ed.; Hamuna Press: Totowa, NJ, 2006.
- (14) Jochems, P.; Satyawali, Y.; Diels, L.; Dejonghe, W. Enzyme Immobilization on/in Polymeric Membranes: Status, Challenges and Perspectives in Biocatalytic Membrane Reactors (BMRs). *Green Chem.* **2011**, *13*, 1609–1623.
- (15) DiCosimo, R.; McAuliffe, J.; Poulouse, A. J.; Bohlmann, G. Industrial Use of Immobilized Enzymes. *Chem. Soc. Rev.* **2013**, *42*, 6437–6474.
- (16) Cantone, S.; Ferrario, V.; Corici, L.; Ebert, C.; Fattor, D.; Spizzo, P.; Gardossi, L. Efficient Immobilisation of Industrial Biocatalysts: Criteria and Constraints for the Selection of Organic Polymeric Carriers and Immobilisation Methods. *Chem. Soc. Rev.* **2013**, *42*, 6262–6276.
- (17) Mannens, G.; Slegers, G.; Lambrecht, R.; Claeys, A. Immobilization of Acetylcoenzyme A Synthetase and the Preparation of an Enzyme Reactor for the Synthesis of [<sup>11</sup>C]Acetylcoenzyme A. *Biochim. Biophys. Acta* **1988**, *959*, 214–219.
- (18) Mannens, G.; Slegers, G.; Lambrecht, R.; Goethals, P. Enzyuatic Synthesis of Carbon-11 Acetyl Coenzue. *J. Labelled Compd. Radiopharm.* **1988**, *XXV*, 695–705.
- (19) Sokic-Lazic, D.; Minteer, S. D. Citric Acid Cycle Biomimic on a Carbon Electrode. *Biosens. Bioelectron.* **2008**, *24*, 945–50.
- (20) Hiroshi, N.; Hitoshi, K.; Isao, T.; Kazutomo, I.; Masaru, K.; Tatsuo, T. Process for producing physiologically active substance by multienzyme process and apparatus for the same. EP0084975 B1, Dec 30, 1986.
- (21) Takagi, K.; Mochizuki, M.; Sakamoto, I.; Teranishi, H. Carriers for immobilization of physiologically active substances. United States Patent, Japan. EP0131369 A2, Jan 16, 1985.
- (22) Dubey, N. C.; Tripathi, B. P.; Stamm, M.; Ionov, L. Smart Core-Shell Microgel Support for Acetyl Coenzyme A Synthetase: A Step Toward Efficient Synthesis of Polyketide-Based Drugs. *Biomacromolecules* **2014**, *15*, 2776–2783.
- (23) Tripathi, B. P.; Dubey, N. C.; Stamm, M. Hollow Microgel Based Ultrathin Thermoresponsive Membranes for Separation, Synthesis, and Catalytic Applications. *ACS Appl. Mater. Interfaces* **2014**, *6*, 17702–17712.
- (24) Kim, J.; Nayak, S.; Lyon, L. A. Bioresponsive Hydrogel Microlenses. *J. Am. Chem. Soc.* **2005**, *127*, 9588–9592.
- (25) Gawlitza, K.; Georgieva, R.; Tavraz, N.; Keller, J.; von Klitzing, R. Immobilization of Water-Soluble HRP within Poly-N-isopropylacrylamide Microgel Particles for Use in Organic Media. *Langmuir* **2013**, *29*, 16002–16009.
- (26) Lu, Y.; Ballauff, M. Thermosensitive Core-Shell Microgels: From Colloidal Model Systems to Nanoreactors. *Prog. Polym. Sci.* **2011**, *36*, 767–792.
- (27) Malmsten, M.; Bysell, H.; Hansson, P. Biomacromolecules in Microgels — Opportunities and Challenges for Drug Delivery. *Curr. Opin. Colloid Interface Sci.* **2010**, *15*, 435–444.

- (28) Ramli, R. A.; Laftah, W. A.; Hashim, S. Core-Shell Polymers: A Review. *RSC Adv.* **2013**, *3*, 15543–15565.
- (29) Doring, A.; Birnbaum, W.; Kuckling, D. Responsive Hydrogels - Structurally and Dimensionally Optimized Smart Frameworks for Applications in Catalysis, Micro-System Technology and Material Science. *Chem. Soc. Rev.* **2013**, *42*, 7391–7420.
- (30) Roy, I.; Gupta, M. N. Smart Polymeric Materials: Emerging Biochemical Applications. *Chem. Biol.* **2003**, *10*, 1161–1171.
- (31) Nayak, S.; Lyon, L. A. Soft Nanotechnology with Soft Nanoparticles. *Angew. Chem., Int. Ed.* **2005**, *44*, 7686–7708.
- (32) Heinz, P.; Brétagne, F.; Mannelli, I.; Sirghi, L.; Valsesia, A.; Ceccone, G.; Gilliland, D.; Landfester, K.; Rauscher, H.; Rossi, F. Poly(N-isopropylacrylamide) Grafted on Plasma-Activated Poly(ethylene oxide): Thermal Response and Interaction With Proteins. *Langmuir* **2008**, *24*, 6166–6175.
- (33) Cayre, O. J.; Chagneux, N.; Biggs, S. Stimulus Responsive Core-Shell Nanoparticles: Synthesis and Applications of Polymer Based Aqueous Systems. *Soft Matter* **2011**, *7*, 2211–2234.
- (34) Matsukata, M.; Aoki, T.; Sanui, K.; Ogata, N.; Kikuchi, A.; Sakurai, Y.; Okano, T. Effect of Molecular Architecture of Poly(N-isopropylacrylamide)-Trypsin Conjugates on Their Solution and Enzymatic Properties. *Bioconjugate Chem.* **1996**, *7*, 96–101.
- (35) Kondo, A.; Fukuda, H. Preparation of Thermo-Sensitive Magnetic Hydrogel Microspheres and Application to Enzyme Immobilization. *J. Ferment. Bioeng.* **1997**, *84*, 337–341.
- (36) Kim, H. K.; Park, T. G. Synthesis and Characterization of Thermally Reversible Bioconjugates Composed of  $\alpha$ -Chymotrypsin and Poly(N-isopropylacrylamide-co-acrylamido-2-deoxy-D-glucose). *Enzyme Microb. Technol.* **1999**, *25*, 31–37.
- (37) Zhang, J.-T.; Petersen, S.; Thunga, M.; Leipold, E.; Weidisch, R.; Liu, X.; Fahr, A.; Jandt, K. D. Micro-Structured Smart Hydrogels with Enhanced Protein Loading and Release Efficiency. *Acta Biomater.* **2010**, *6*, 1297–1306.
- (38) Shamim, N.; Liang, H.; Hidajat, K.; Uddin, M. S. Adsorption, Desorption, and Conformational Changes of Lysozyme from Thermosensitive Nanomagnetic Particles. *J. Colloid Interface Sci.* **2008**, *320*, 15–21.
- (39) Ballauff, M.; Lu, Y. “Smart” Nanoparticles: Preparation, Characterization and Applications. *Polymer* **2007**, *48*, 1815–1823.
- (40) Welsch, N.; Wittemann, A.; Ballauff, M. Enhanced Activity of Enzymes Immobilized in Thermoresponsive Core-Shell Microgels. *J. Phys. Chem. B* **2009**, *113*, 16039–16045.
- (41) Barbosa, O.; Torres, R.; Ortiz, C.; Berenguer-Murcia, Á.; Rodrigues, R. C.; Fernandez-Lafuente, R. Heterofunctional Supports in Enzyme Immobilization: From Traditional Immobilization Protocols to Opportunities in Tuning Enzyme Properties. *Biomacromolecules* **2013**, *14*, 2433–2462.
- (42) Fernandez-Lafuente, R. Stabilization of Multimeric Enzymes: Strategies to Prevent Subunit Dissociation. *Enzyme Microb. Technol.* **2009**, *45*, 405–418.
- (43) Rodrigues, R. C.; Ortiz, C.; Berenguer-Murcia, A.; Torres, R.; Fernandez-Lafuente, R. Modifying Enzyme Activity and Selectivity by Immobilization. *Chem. Soc. Rev.* **2013**, *42*, 6290–6307.
- (44) Bahulekar, R.; Ayyangar, N. R.; Ponrathnam, S. Polyethyleneimine in Immobilization of Biocatalysts. *Enzyme Microb. Technol.* **1991**, *13*, 858–868.
- (45) Zhu, J.; Tang, A.; Law, L. P.; Feng, M.; Ho, K. M.; Lee, D. K. L.; Harris, F. W.; Li, P. Amphiphilic Core-Shell Nanoparticles with Poly(ethylenimine) Shells as Potential Gene Delivery Carriers. *Bioconjugate Chem.* **2004**, *16*, 139–146.
- (46) Pessela, B. C. C.; Fernández-Lafuente, R.; Fuentes, M.; Vián, A.; García, J. L.; Carrascosa, A. V.; Mateo, C.; Guisán, J. M. Reversible Immobilization of A Thermophilic B-Galactosidase via Ionic Adsorption on PEI-Coated Sepabeads. *Enzyme Microb. Technol.* **2003**, *32*, 369–374.
- (47) Leung, M. F.; Zhu, J.; Harris, F. W.; Li, P. New Route to Smart Core-Shell Polymeric Microgels: Synthesis and Properties. *Macromol. Rapid Commun.* **2004**, *25*, 1819–1823.
- (48) Xu, J.; Zeng, F.; Wu, S.; Liu, X.; Hou, C.; Tong, Z. Gold Nanoparticles Bound on Microgel Particles and their Application as an Enzyme Support. *Nanotechnology* **2007**, *18*, 265704.
- (49) Webster, L. T. Studies of the Acetyl Coenzyme A Synthetase Reaction: V. The Requirement for Monovalent and Divalent Cations in Partial Reactions involving Enzyme-bound Acetyl Adenylate. *J. Biol. Chem.* **1967**, *242*, 1232–1240.
- (50) Pettersson, H.; Olsson, P.; Bülow, L.; Pettersson, G. Kinetics of the Coupled Reaction Catalysed by a Fusion Protein of Yeast Mitochondrial Malate Dehydrogenase and Citrate Synthase. *Eur. J. Biochem.* **2000**, *267*, 5041–5046.
- (51) Zhang, Q.; Ghosh, S.; Samitsu, S.; Peng, X.; Ichinose, I. Ultrathin Freestanding Nanoporous Membranes Prepared from Polystyrene Nanoparticles. *J. Mater. Chem.* **2011**, *21*, 1684–1688.
- (52) Leung, M. F. *Novel Smart Core-Shell microgels: Synthesis, Characterization and Application*; The Hong Kong Polytechnic University: Hong Kong, 2006.
- (53) Pelton, R. Temperature-Sensitive Aqueous Microgels. *Adv. Colloid Interface Sci.* **2000**, *85*, 1–33.
- (54) Cullen, S. P.; Mandel, I. C.; Gopalan, P. Surface-Anchored Poly(2-vinyl-4,4-dimethyl azlactone) Brushes as Templates for Enzyme Immobilization. *Langmuir* **2008**, *24*, 13701–13709.
- (55) Frenkel, E. P.; Kitchens, R. L. Purification and Properties of Acetyl Coenzyme A Synthetase from Bakers’ Yeast. *J. Biol. Chem.* **1977**, *252*, 504–507.
- (56) del-Val, M. I.; Otero, C. Kinetic and Spectroscopic Behaviour of a Lipase-Microgel Derivative in Aqueous and Micellar Media. *J. Mol. Catal. B: Enzym.* **1998**, *4*, 137–147.
- (57) Satyanarayana, T.; Klein, H. P. Studies on Acetyl-Coenzyme A Synthetase of Yeast: Inhibition by Long-Chain Acyl-Coenzyme A Esters. *J. Bacteriol.* **1973**, *115*, 600–606.
- (58) Eisenthal, R.; Danson, M. J.; Hough, D. W. Catalytic Efficiency and  $k_{cat}/K_M$ : a Useful Comparator? *Trends Biotechnol.* **2007**, *25*, 247–249.
- (59) Yasui, M.; Shiroya, T.; Fujimoto, K.; Kawaguchi, H. Activity of Enzymes Immobilized on Microspheres with Thermosensitive Hairs. *Colloids Surf., B* **1997**, *8*, 311–319.
- (60) Shakya, A. K.; Sami, H.; Srivastava, A.; Kumar, A. Stability of Responsive Polymer-Protein Bioconjugates. *Prog. Polym. Sci.* **2010**, *35*, 459–486.
- (61) Haupt, B.; Neumann, T.; Wittemann, A.; Ballauff, M. Activity of Enzymes Immobilized in Colloidal Spherical Polyelectrolyte Brushes. *Biomacromolecules* **2005**, *6*, 948–955.
- (62) Park, T. G.; Hoffman, A. S. Thermal Cycling Effects on the Bioreactor Performances of Immobilized Beta-Galactosidase in Temperature-Sensitive Hydrogel Beads. *Enzyme Microb. Technol.* **1993**, *15*, 476–482.